# Calculation, Simulation, and Testing for the Natural Frequency of a Micro Accelerometer*

Xiong Jijun, Fan Bo†, Guo Hugang, and Gao Jianfei

(*National Key Laboratory for Electronic Measurement Technology, Key Laboratory of Instrumentation Science & Dynamic Measurement of the Ministry of Education, North University of China, Taiyuan 030051, China*)

**Abstract**: A calculation and test method for the natural frequency of a high-*g* micro accelerometer with complex structures is presented. A universal formula for natural frequency, which can significantly simplify the structural design process, is deduced and confirmed by experiment. A simplified analytical model is established to describe the accelerometer's mechanical behavior and deduce the formula for the natural frequency. Finite element modeling is also conducted to evaluate the natural frequency of the micro-accelerometer and verify the formula. The results obtained from the analytical model and the finite element simulation show good agreement. Finally, a shock comparison method designed for acquiring the high frequency characteristics of the accelerometer is introduced to verify the formula by testing its actual natural frequency.

**Key words**: natural frequency; micro accelerometer; Rayleigh-Ritz formula
**EEACC**: 7230
**CLC number**: TM302 **Document code**: A **Article ID**: 0253-4177(2008)09-1715-08

## 1 Introduction

With the development of the micro-machining technique, research on the micro-accelerometer is increasing. Because of its advantages such as simple structure, easily to detect signals, and mature fabrication process, the piezoresistive accelerometer has long held people's attention[1,2]. However, most piezoresistive accelerometers have poor dynamic behavior. Even worse, some are damaged after the first test. Analysis indicates the reason is that resonance occurs when additional dynamic load containing the frequency component equals or nears the system's natural frequency. It induces such a large displacement of the mass that the component structure is damaged. Two solutions can be adopted to avoid this. One is to fill the viscous fluid in the system to reduce the structure's vibration amplitude using the damping force of fluid[3]. The other is to enhance the component natural frequency as high as possible, but at the cost of decreasing the system's sensitivity.

Here we adopt the latter. To acquire better dynamic performance, the system's natural frequency and sensitivity should be selected eclectically, so as to scheme out an optimal structure. However, the calculation of natural frequency in complex structures is complicated. There is no universal formula to be used. In general, the natural frequency has to be determined by computer simulation. Accordingly, special structural models for simulation must be established first. Then the natural frequency is derived by simulation and the structure is optimized based on it. This increases the work load greatly. Moreover, it is impossible to establish a structural model for various sizes. So the simulation has to be carried out on the basis of an approximate model and the acquired final structural model may not be the best one. In summary, it is meaningful to deduce a general calculation formula to simplify the design process.

In this paper, a deduction method of the natural frequency formula is presented by taking a piezoresistive accelerometer with a four side eight-beam structure as a case study.

## 2 Solution of the natural frequency

The structural model must be simplified before solving the first eigenfrequencies of the accelerometer.

Figure 1 (a) shows the accelerometer sketch of the four side eight-beam-mass structure. The structure model is simplified so as to facilitate the stress analysis[4].

(1) First, the eight-beam-mass structure (Fig. 1 (a)) is simplified to a four-beam-mass structure. The

* Project supported by the National Natural Science Foundation of China (No. 50775209) and NCET
† Corresponding author. Email: fanbo46@163.com
Received 8 March 2008, revised manuscript received 21 April 2008

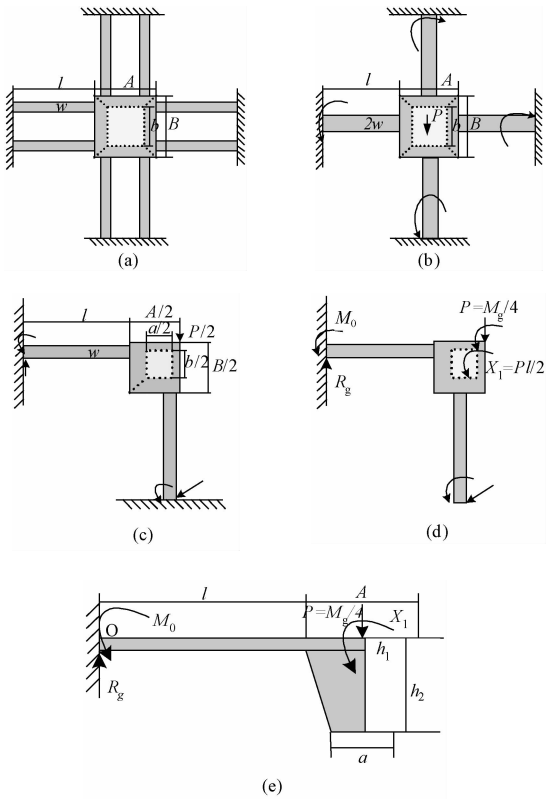


Fig. 1 Simplified model of the structure (a) Four sides eight beam structure; (b) Four beams structure; (c) Two beams structure; (d) Remove redundant constraints; (e) Final simplified structure

structure and its load distribution are shown in Fig. 1 (b), in which the width of the beams is doubled.

(2) Because the four-beam-mass structure is completely symmetric about the *xoy* coordinate plane, it can be transformed to a two beam structure, as shown in Fig. 1 (c).

(3) After shedding redundant constraints, the structural force distribution is shown in Fig. 1 (d).

(4) The effect of the bending moment at the free end in the bending deformation can be neglected because of its fixed beam structure.

The final simplified structure is shown in Fig. 1 (e).

Figure 1 (e) shows that the solution of the structural natural frequency is a statically indeterminable problem. So the regular equation for force method is utilized,

$$\delta_{11} X_1 + \Delta_{1P} = 0 \tag{1}$$

where $\delta_{11}$ is the displacement of the action spot along the action direction when redundant restraint load $X_1 = 1$ is applied, and $\Delta_{1P}$ is the displacement at the free end of the beam when the applied load $P$ functions independently, $P = \frac{M_g}{4}$, $L = l + \frac{A}{2}$. Moreover,

$$\delta_{ij} = \sum_{k=1}^{2} \int_k \frac{M_i^0 M_j^0}{EI} \mathrm{d}x \tag{2}$$

$$\Delta_{iP} = \sum_{k=1}^{2} \int_k \frac{M_i^0 M_P}{EI} \mathrm{d}x \tag{3}$$

where $M_P$ is the bending moment when the outside load functions independently, $M_i^0$ is the bending moment when the outside load $X_i = 1$ functions independently, and $l_k$ is the beam length of the linkage system.

Combining the simplified structure above, when the outside load $P$ functions independently, the bending moment at point $A$ is:

$$M_P = P(x - l), \quad 0 \leqslant x \leqslant l \tag{4}$$

When the outside load $X_1 = 1$ functions independently, the bending moment of $A$ is:

$$M_1^0 = 1, \quad 0 \leqslant x \leqslant l \tag{5}$$

Then,

$$\Delta_{1P} = \int \frac{M_1^0 M_P}{EI} \mathrm{d}x = -\frac{Pl^2}{2EI} \tag{6}$$

$$X_1 = -\frac{\Delta_{1P}}{\delta_{11}} = \frac{pl}{2} \tag{7}$$

The force and bending moment at the fixed point of O is:

$$R_o = P = \frac{1}{4} M_g \tag{8}$$

$$M_0 = \frac{Pl}{2} \tag{9}$$

Meanwhile, based on the structural force distribution (Fig. 1 (b)), the rotary inertia of the elastic beam is:

$$I = \frac{wh_1^3}{6} \tag{10}$$

The first-order mode shape of the accelerometer is such that the mass makes the translation along the $z$ direction and the four beams have an identical deflection. So the beam deflection can be obtained by the stress analysis of any beam, as shown in Fig. 1(e).

The deflection of beams was computed by the superposition method (where $P = \frac{Ma}{4}$, $L = l + \frac{A}{2}$). When the outside load $P$ functions independently, the deflection equation of the beam is:

$$y_1(x) = -\frac{Px^2}{6EI}(3l - x), \quad 0 \leqslant x \leqslant l \tag{11}$$

When the outside load $X_1$ functions independently, the deflection equation of the beam is:

$$y_2(x) = \frac{Px^2 l}{4EI}, \quad 0 \leqslant x \leqslant l \tag{12}$$

Hence, the total deflection of the beam is:

$$y(x) = y_1(x) + y_2(x) = \frac{Px^2(2x - 3l)}{12EI}, \quad 0 \leqslant x \leqslant l \tag{13}$$

The natural frequency can be calculated with the Rayleigh-Ritz formula[5],

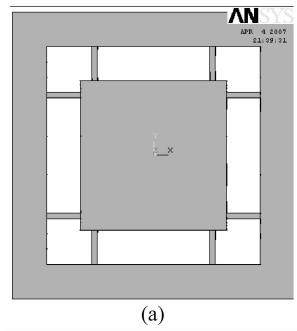

(a)

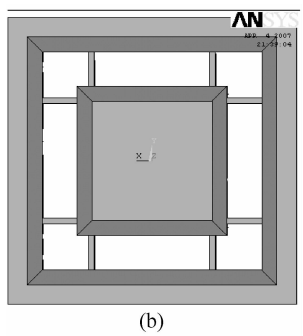

(b)

Fig. 2　FEA model of the accelerometer　(a) Front face; (b) Back side

where $M$ is the weight of the mass, $E$ is the Young's-modulus of the material, $I$ is the inertia moment of the elastic beam, $l$ is the length of the beam, $w$ is the width of the beam, $h_1$ is the thickness of the beam, $h_2$ is the thickness of the mass, and $P$ is the external force on the mass.

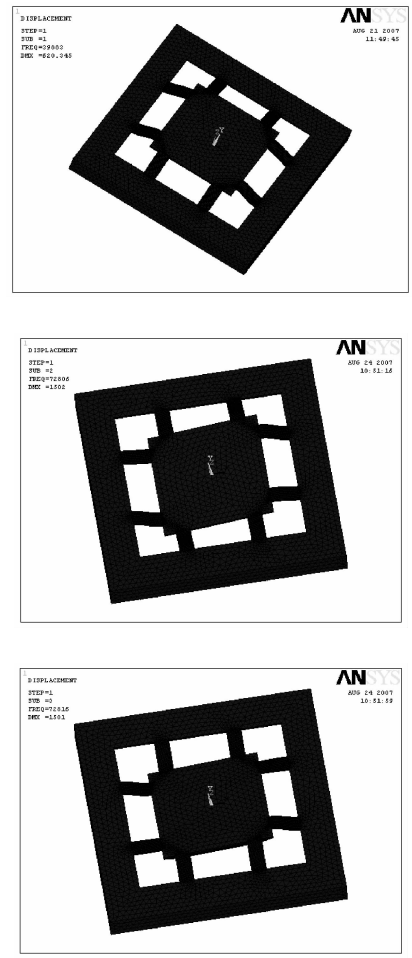

Fig. 3　FEM simulation results for the resonance frequency

$$w_s^2 = \frac{\int_0^L EIy''^2(x)\mathrm{d}x}{\int_0^L \rho WHy^2(x)\mathrm{d}x}$$

$$= \frac{\int_0^l EI_1 y''^2(x)\mathrm{d}x + \int_l^{A/2+I} 0\mathrm{d}x}{\int_0^l \rho w h_1 y^2(x)\mathrm{d}x + \int_l^{l+\frac{A-a}{2}} \rho \frac{b+B}{4}[h_1 + (x-l)\tan\theta]y^2(l)\mathrm{d}x + \int_{l+\frac{A-a}{2}}^{l+\frac{A-a}{2}+\frac{a}{2}} \rho \frac{b+B}{4} h_2 y^2(l)\mathrm{d}x}$$

$$\approx \frac{\int_0^l EI_1 y''^2(x)\mathrm{d}x}{\int_0^l \rho w h_1 y^2(x)\mathrm{d}x + \frac{1}{4}My^2(l)} \tag{14}$$

## 3　Simulation and verification

The beam-mass structural natural frequencies are simulated by the finite element analysis software ANSYS[6]. In the simulation, the accelerometer structural model, which consists of eight beams and a mass, is established first, as shown in Fig. 2. Suppose the dimensions of the mass are $A = 1900\mu$m, $B = 1900\mu$m, $h_2 = 395\mu$m, and the length, width, thickness of the beam are 500, 250, and 40$\mu$m, respectively.

Figure 3 and Table 1 show the simulation results of the variation rate and the natural frequency.

Then, we change the parameters of the beams. First, we regard the width of the beams as constants ($w = 250\mu$m), and the depth of the beam as variables ($h_1 = 20 \sim 60\mu$m). Then, we regard the thickness of the beams as constants ($h_1 = 40\mu$m) and the width of the beams as variables ($w = 100 \sim 500\mu$m).

Finally, the natural frequencies of structural different parameters are acquired by Eq. (14).

Table 1　Summary of FEM simulation

| | |
|---|---|
| Resonance frequency/kHz | 1st mode: 39.88<br>2nd mode: 72.81<br>3rd mode: 72.82 |

Table 2 Results of the simulation and calculation

| Mass/$\mu$m | | | Beam/$\mu$m | | | Natural frequency/Hz | |
|---|---|---|---|---|---|---|---|
| Length | Width | Thickness | Length | Width | Thickness | Simulation | Calculation |
| 1900 | 1900 | 395 | 500 | 250 | 20 | 14127 | 13598.9 |
| | | | | | 30 | 26562 | 25966.7 |
| | | | | | 40 | 39883 | 39413.9 |
| | | | | | 50 | 53632 | 53650.3 |
| | | | | | 60 | 66883 | 66480.6 |
| | | | | | 70 | 80299 | 80757.1 |
| | | | | 100 | 40 | 26073 | 24332.9 |
| | | | | 150 | | 31445 | 29786.2 |
| | | | | 200 | | 35914 | 34376.2 |
| | | | | 250 | | 39883 | 38413.9 |
| | | | | 300 | | 43295 | 42058.5 |
| | | | | 350 | | 46468 | 45404.9 |
| | | | | 400 | | 49433 | 48500.8 |
| | | | | 500 | | 54824 | 54085.2 |

The simulation and calculation results are summarized in Table 2. These results indicate that the natural frequency of the calculation nearly coincided with those of the simulation and the error is 3.77%, as shown in Fig. 4.

## 4 Tested accelerometer

The tested piezoresistive accelerometer has the same structure as the simulated model, which is designed by North University of China. Figure 5 shows the structure of the sensor and reveals that the whole structure is completely asymmetric in the *xoy* plane. Considering the present micromachining techniques in China, we set the size of the accelerometer as: a beam width of 250$\mu$m; beam length of 500$\mu$m; beam thickness of 40$\mu$m; mass width of 1900$\mu$m; mass thickness of 395$\mu$m. Its measurement range is 0～50000g. The frequency response range is over 30kHz, in accordance with that calculated by Eq. (14), which is 38.41kHz.

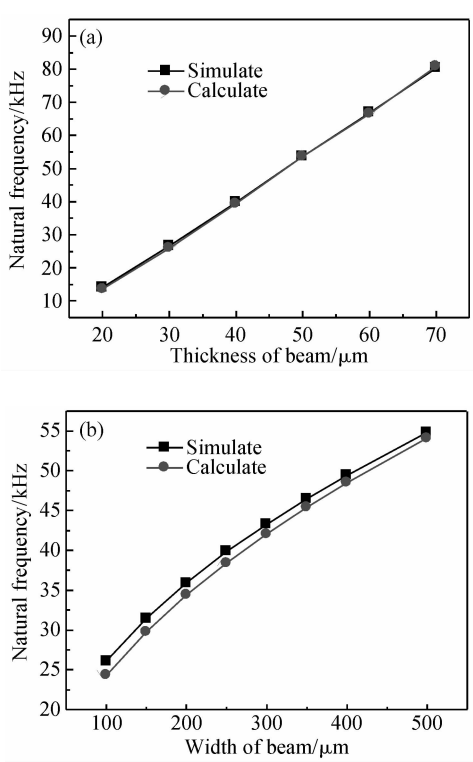


Fig. 4 Nature frequency of simulation and calculation

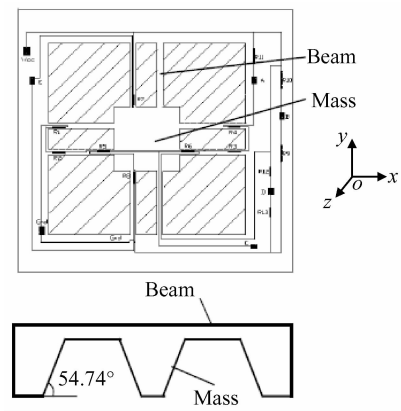


Fig. 5 Eight-beam-mass structure and piezoresistors

The accelerometer is fabricated using a bulk silicon fabrication process with diffused piezoresistors as sensing elements. On the top surface of the beams as well as the frame, 13 diffused piezoresistors are formed to construct three Wheatstone bridges, which detect the accelerations along the *z*-, *x*-, and *y*-axis, respectively. The Wheatstone bridges are shown in Fig. 6, in which the values of the piezoresistors are as follows.

$$R_1 = R_2 = R_3 = R_4 = R_5 = R_6 = R_8 = R_{12} = R_{13} = 2\text{k}\Omega$$

$$R_9 = R_{10} = R_{11} = 8\text{k}\Omega$$

During the penetration process, the mass of the structure vibrates, subsequently, the beams bends as a result of strain distribution. This results in stress distribution along the beams, and finally, the stress distribution causes the variations of piezoresistors.

To fabricate such a high-*g* three-axis micro accelerometer, bulk silicon micromachining techniques are used. To start the fabrication process, a 100mm n-type (100) double polished silicon wafer with a thickness

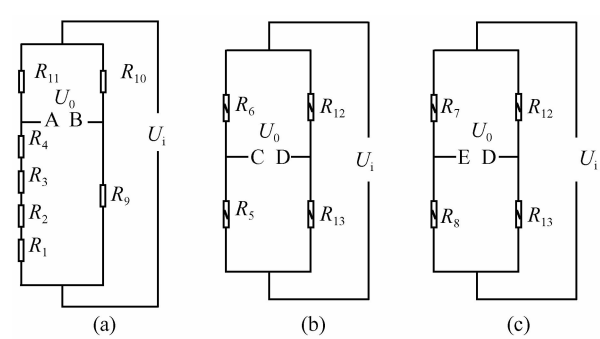


Fig. 6 Wheatstone bridge circuits (a) *z*-axis; (b) *x*-axis; (c) *y*-axis

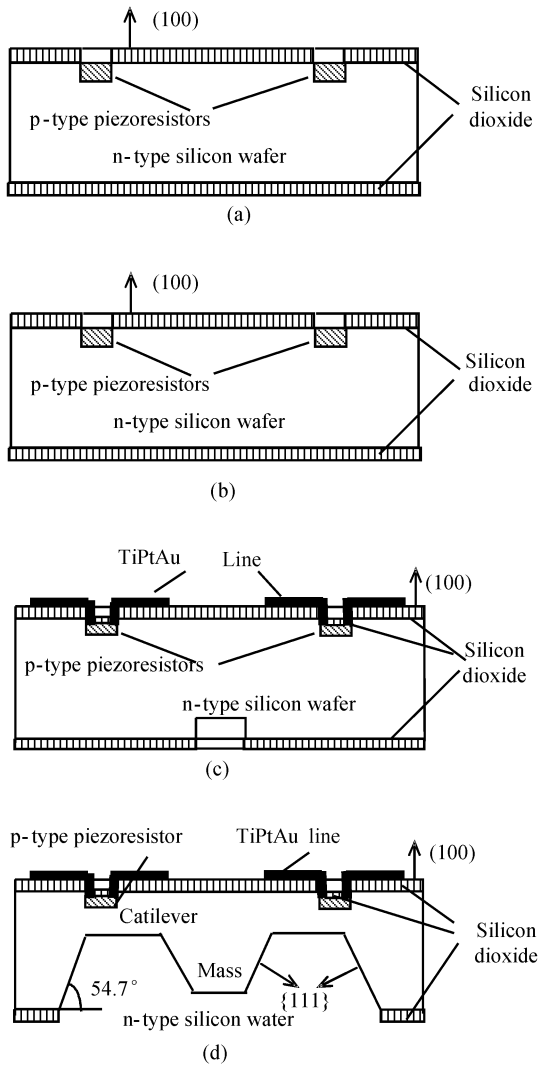


Fig. 7　Fabrication process of the three-axis accelerometer (a) Phosphorus injecting to form the n-type piezoresistors; (b) Front photolithography to make connecting holes; (c) RIE etching, TiPtAu evaporation, and liftoff; (d) Back side KOH wet etching

of 400$\mu$m is prepared. First an ion implantation is adopted to inject phosphorus (P) into silicon to form n-type piezoresistors; second, front photolithography is adopted for the evaporation and liftoff step to form the connecting wires; then an RIE etching is carried out at the back of the silicon to make a hole, which is used to do the back grind on the mass to obtain a thickness of 395$\mu$m; an KOH etching step is put forward to form the mass, and the KOH etching will form an angle of 54.74°, as shown in Fig. 5. Finally, the whole structure is released by an ICP step, the etching depth of which is 40$\mu$m, equaling the thickness of the beams. Figure 7 illustrates the fabrication process of this structure. Figure 8 shows the photos of the three-axis accelerometer after the fabrication process and a photo of the packaged accelerometer.

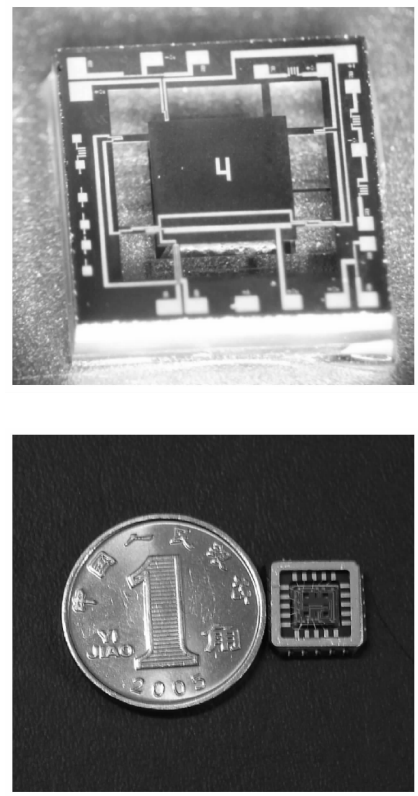

Fig. 8　SEM of the structure and photo of a packaged accelerometer

## 5　Experimental verification

The formula for calculating the Natural frequency is verified by testing. Because the general vibration table has a limited sweep frequency scope (zero to several kilohertz) and very small vibration amplitude, significant errors may arise when testing the frequency response of the high-$g$ accelerometer, which leads to the wrong analysis results of the steady-resonance characteristics. In this experiment, it is impractical to test the sweep frequency characteristic with the traditional shaking table. Therefore, the shock comparison method is introduced.

### 5.1　Principles of the shock comparison method[7,8]

The tested accelerometer and the standard sensor are installed back-to-back in the shocking-excitation device. As shown in Fig. 9, when a transient pulse $u(t)$ is applied by the excitation device, the two sensors will produce the responses $x(t)$, $y(t)$, respectively. Suppose the sensor system is the linear steady link, the frequency domain response can be written as

$$\begin{aligned} Y(s) &= H_b(s)U(s) \\ X(s) &= H_a(s)U(s) \end{aligned} \tag{15}$$

where $H_a(s)$ and $H_b(s)$ are the transfer functions of the standard sensor and the tested sensor. Consequently,

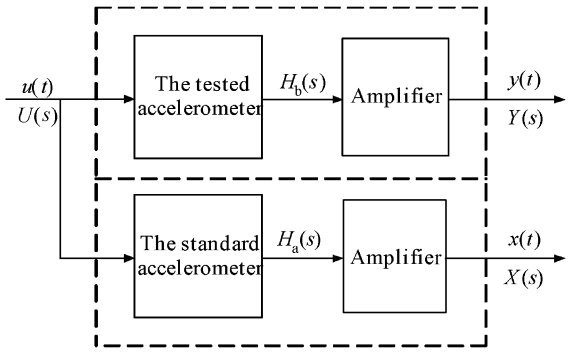


Fig. 9 Principle block diagram of the shock comparison method for frequency characteristics

$$Y(s)/X(s) = H_b(s)/H_a(s)$$

There is:

$$H_b(s) = H_a(s)\frac{Y(s)}{X(s)} \tag{16}$$

Given that the Fourier Transform of $x(t)$ and $y(t)$ exist, they become $X(jw)$ and $Y(jw)$, respectively. Let $Y(jw)/X(jw) = H(jw) = A(w)e^{j\varphi(w)}$, $H_a(jw) = A_a(w)e^{j\varphi_a(w)}$, $H_b(jw) = A_b(w)e^{j\varphi_b(w)}$, Thus,

$$H_b(jw) = H_a(jw)H(jw) \tag{17}$$

If the frequency characteristic of the standard sensor is known, the frequency characteristic of the tested accelerometer $H_b(jw)$ is obtained by Eq. (17). When the work frequency range of the standard sensor sufficiently covers that of the tested accelerometer, $A_a(w) \equiv K$, $\varphi_a = 0$. Let $K = 1$. Thus,

$$H_b(jw) = H(jw) \tag{18}$$

Then the frequency characteristic of the tested accelerometer can be determined and the natural frequency is easily obtained.

### 5.2 Experiment and results

By means of a calibrated shocking hammer, experiments are done to verify the formula. The test principle is that the hammer smites the fixed platform under the pull of gravity so that the test objects undergo a great acceleration stress of 200～50000g. As shown in Fig. 10, the tested accelerometer and the standard sensor are installed in the shocking hammer. Figure 11 shows the schematic diagram of the shocking hammer experimental system.

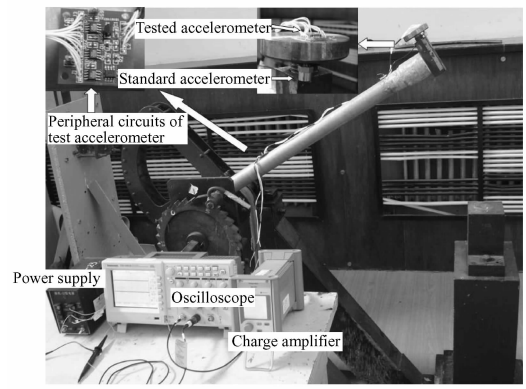


Fig. 10 Shocking hammer experimental system

The output charge signal of the standard sensor is transformed to a voltage signal by the 5015 charge amplifier from Kistler Inc.[9]. The output voltage signal of the tested accelerometer is amplified by its signal conditioning circuit. Then their waveforms and data are collected by a TDS 1001B oscilloscope from Tektronix Inc.[10]. Figure 12 shows the experimental results.

Based on the least square method of the analysis software ORIGINPRO 7.5[11,12], substituting the experimental data into Eq. (23), the transfer function of the tested accelerometer is deleted.

$$H_b = \frac{0.141\times10^{10}s^2 + 0.367\times10^{14}s + 0.333\times10^{19}}{0.237\times10^{10}s^2 + 0.154\times10^{14}s + 0.333\times10^{19}} \tag{19}$$

Figure 13 shows the Bode diagram drawn by Eq. (19), from which the resonance frequency of the tested high-$g$ accelerometer can be obtained.

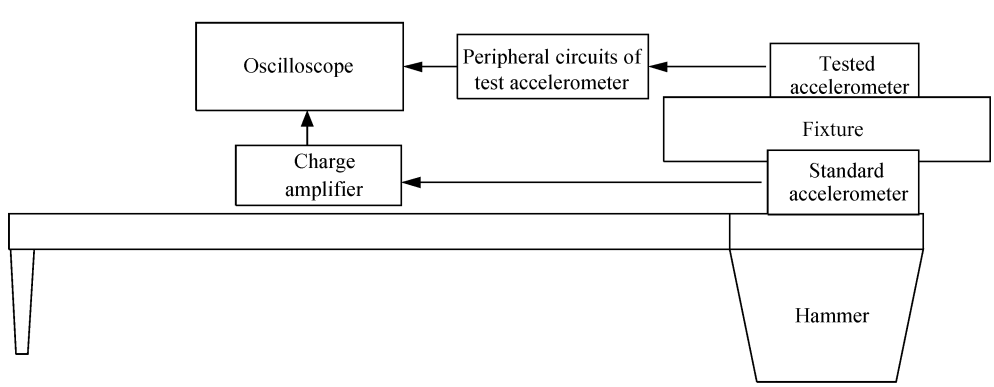


Fig. 11 Schematic diagram of the shocking hammer experimental system

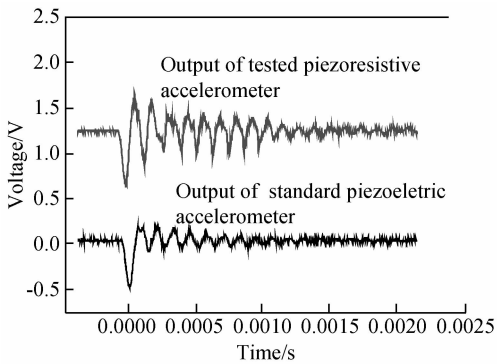


Fig. 12　Waveforms in shock test of two sensors

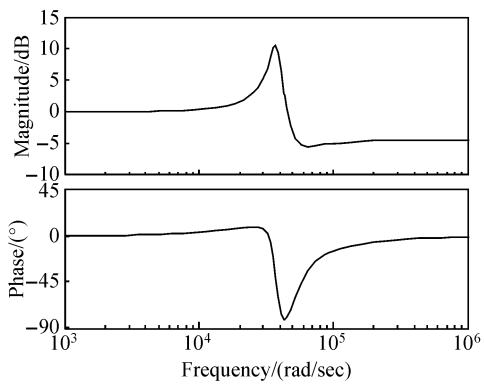


Fig. 13　Bode diagram of the tested accelerometer

$$w_r = 37.2\text{kHz} \tag{20}$$

By definition, the damping ratio is $\xi = 0.25$, so the natural frequency is:

$$w_n = w_r/\sqrt{1-\xi^2} = 38.42\text{kHz} \tag{21}$$

The experiment results are consistent with the theoretically calculated value from the formula. Thus, the theoretical formula of natural frequency is applicable to solve the natural frequency of the accelerometer.

## 6　Conclusion

The theoretical calculation formula for the natural frequency was deduced and verified by simulation and experiment. We can draw the following conclusions:

(1) The method for deducing the calculation formula introduced in this paper is only suitable for the comparative complex beam-mass structure because the mass was treated as a rigid body and the shear deformation and the tensional deformation of the structure are neglected to simplify the structure and facilitate the establishment of mechanical equation. When applied in other cases, the deduction method has great deviation.

(2) The natural frequency calculated using the formula agrees well with the simulation results and experimental data. Accordingly, the simplification method can fit any MEMS components with a complex beam-mass structure and its natural frequency can be obtained by the deduced formula.

(3) In the validation test, the dynamic calibration method in the time domain is used. Comparison indicates it is feasible to acquire the natural frequency of the high-$g$ acceleration by the shock comparison method.

### References

[1] Macdonald G A. A review of low cost accelerate for vehicle dynamics. Sensors and Actuators, 1990, A21～A23: 303
[2] Suminto T. A simple high performance piezoresistive accelerometer. Tech Digest of 7th Int Conf Solid-State Sensors and Actuators, San Francisco, CA, USA, 1991: 104
[3] Wang Z, Zong D, Lu D, et al. A silicon micromachined shock accelerometer with twin-mass-plate structure. Sensors and Actuators, 2003, A107: 50
[4] Wang Fuxing, Sun Huadong. Mechanics of materials. Beijing: Enginery industrial publishing company, 2001
[5] Timoshenko S. Vibration problems in engineering. 4th ed. John Wiley and Sons, Inc, 1974: 22
[6] Tschan T, Rooij N, Bezinge A. Analytical and FEM modeling of piezoresistive silicon accelerometers: predictions and limitations compared to experiments. Sensors Mater, 1992, 3(4): 189
[7] Huan Junqin. A practical modeling method for static and dynamic data processing. Beijing: Enginery Industrial Publishing Company, 1988
[8] Huan Junqin. Dynamics test system. Beijing: National Defense Industry Publishing Company, 1996
[9] http://www.kistler.com/
[10] http://www.tek.com/
[11] Fang Anping. Analysis and exploit data of Origin 7.5. Beijing: Enginery Industrial Publishing Company, 2006
[12] Zhou Jianping. Origin practical course. Xi'an Communication University Publishing Company, 2007

# 微加速计固有频率的推导及验证*

熊继军 范 波† 郭虎岗 高建飞

（中北大学电子测试技术国家重点实验室，仪器科学与动态测试教育部重点实验室，太原 030051）

**摘要**：为了解决压阻式加速度计的动态特性欠佳的共性，避免微加速度计在工作过程中因为共振导致结构损坏，在结构设计过程中选择合理固有频率是至关重要的.文中针对一种四边八梁结构的高 $g$ 值压阻式加速度计，通过力学知识，简化结构并推导出其固有频率的理论计算公式，利用有限元仿真软件和测试高 $g$ 值加速度计频率特性的方法，对该理论公式进行了仿真和实验验证，证明该理论公式的正确性和可用性.同时，文中介绍的简化结构的模型，能够用于复杂结构的应力、应变等的求解，验证的实验方法可以用于高 $g$ 值加速度计固有频率的测试.而且，在加速度计结构的设计过程中，直接利用固有频率公式计算出结构的固有频率，从而简化加速度计的结构设计和优化过程，设计出最合理的固有频率结构.

**关键词**：固有频率；微加速度计；Rayleigh-Ritz 公式

**EEACC**：7230

**中图分类号**：TM302 **文献标识码**：A **文章编号**：0253-4177(2008)09-1715-08

* 国家自然科学基金(批准号:50775209)及 NCET 资助项目

† 通信作者.Email:fanbo46@163.com

2008-03-08 收到，2008-04-21 定稿